

LightRing: Always-Available 2D Input on Any Surface

Wolf Kienzle, Ken Hinckley
Microsoft Research
One Microsoft Way, Redmond, WA 98052
{wkienzle,kenh}@microsoft.com

ABSTRACT

We present *LightRing*, a wearable sensor in a ring form factor that senses the 2d location of a fingertip on any surface, independent of orientation or material. The device consists of an infrared proximity sensor for measuring finger flexion and a 1-axis gyroscope for measuring finger rotation. Notably, *LightRing* tracks subtle fingertip movements from the finger *base* without requiring instrumentation of other body parts or the environment. This keeps the normal hand function intact and allows for a socially acceptable appearance. We evaluate *LightRing* in a 2d pointing experiment in two scenarios: on a desk while sitting down, and on the leg while standing. Our results indicate that the device has potential to enable a variety of rich mobile input scenarios.

Author Keywords

Mobile, input, sensors, wearable, finger, ring

ACM Classification Keywords

H.5.2. [Information interfaces and presentation]: User Interfaces—Graphical user interfaces; Input devices and strategies

INTRODUCTION

The increasing ubiquity of computing devices has created a demand for data input techniques that are *always-available* [9]. Wearable devices naturally meet this requirement and are gaining popularity for simple control tasks, for example, to skip tracks or change volume on a music player. Unfortunately, always-available input remains a largely unsolved problem for richer applications, such as text entry or web browsing, which typically require accurate 2d pointing or stroke input.

In this paper we propose *LightRing* (Fig. 1), a small input device that is worn on the finger and tracks 2d fingertip movements while the hand rests on any surface, regardless of orientation or material.

Paste the appropriate copyright/license statement here. ACM now supports three different publication options:

- ACM copyright: ACM holds the copyright on the work. This is the historical approach.
- License: The author(s) retain copyright, but ACM receives an exclusive publication license.
- Open Access: The author(s) wish to pay for the work to be open access. The additional fee must be paid to ACM.

This text field is large enough to hold the appropriate release statement assuming it is single-spaced in TimesNewRoman 8 point font. Please do not change or modify the size of this text box.

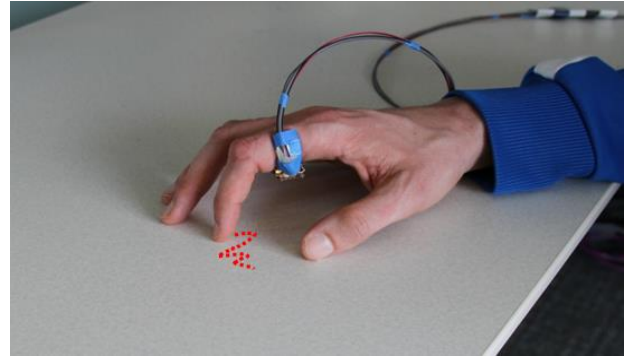


Figure 1. *LightRing* tracks the 2d position of a fingertip on any surface.

Previous finger-worn devices for 2d input include *MIDS* [7], which tracks the fingertip with accelerometers on the finger. *MagicFinger* [13] uses an optical flow sensor (as used in optical mice) attached to the finger for 2d tracking. *FingerPad* [2] and *uTrack* [3] instrument the fingertip with a small (passive) magnet, and a second finger with an active device that tracks the finger by magnetic field changes.

Unfortunately, these solutions cannot be worn at the finger *base* but require instrumentation of a lower finger segment. Compared to an ordinary ring (e.g. a wedding band) such devices have a higher risk of interfering with the normal hand function, and are therefore facing a hurdle for wide adoption and social acceptance.

The key contribution of *LightRing* is a solution to the fundamental problem of sensing fine-grained, subtle fingertip motion *from the finger base* with a very simple and small device that looks and feels like an ordinary ring.

HARDWARE

Our hardware prototype (Fig. 2, left) consists of a plastic ring and two simple sensors. The first sensor is a 1-axis gyroscope. We use a *Sparkfun* board with an *IvenSense ITG-3200* gyroscope that has three axes, but we only use the rotation rate $d\Phi$ in the plane of the red circuit board as illustrated in Fig. 2 (left). Note that the board also has an accelerometer on it, which we currently do *not* use.

The second sensor consists of an infrared emitter (*Osram SFH4550*) and detector (*Honeywell SD5410*). Together, these serve as a proximity sensor: the amount of IR light seen by the detector relates to the distance between the ring and the middle segment (*middle phalanx*) of the instrumented finger. Assuming Lambertian reflectance of the skin, the light intensity should fall off quadratically with

distance (*inverse square law*). This distance changes when the finger is flexed or extended. The emitter and detector parts were chosen to have a narrow viewing angle (6° and 12° , respectively) to prevent spurious reflections from other fingers or the input surface. To suppress ambient lighting changes we measure distance by first registering the detector output with the LED *off*, and then subtracting this value from the output with the LED *on* (after 1 millisecond). We refer to the measured value as \mathbf{d} .

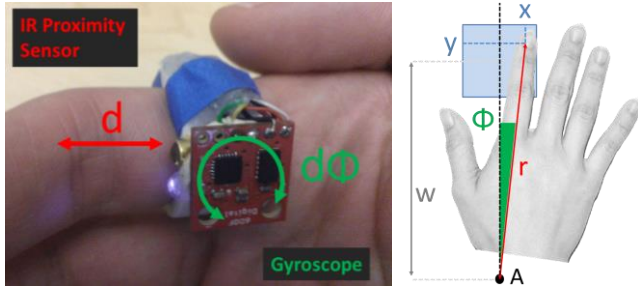


Figure 2. (Left) Sensor hardware. The “blue” light from the IR emitter is invisible to the human eye. (Right) Fingertip position (x, y) in wrist coordinates (blue square) and its corresponding angle Φ and radius r . The dashed black line denotes $x = \Phi = 0$, the current “up” direction.

The ring is wired to an Arduino UNO board. The sensors run at 50Hz which we found sufficient for our application. The sampling resolution of the gyroscope part is 14bit, the proximity values are read by the analog input on the Arduino UNO, which uses a 10bit ADC.

This setup suffices for evaluating 2d pointing precision and speed in a user experiment. Real-world applications will likely require adding a button to the ring, for example, on the side where it can be tapped with the thumb. Also, the simple hardware design should lend itself well to making the ring battery-powered and wireless.

It should be noted that optical sensors have been proposed for measuring finger flexion in wrist-worn devices as well [1][5][6][10]. Those systems typically offer more degrees of freedom (e.g. recover full hand pose [6]), much like to glove-based input devices [12], but are also more complex.

INPUT METHOD

The sensor hardware described above can track subtle fingertip locations on any surface as follows. First, the user rests the wrist (*carpus*) the surface (Fig. 1). Then, the tip of the instrumented finger is moved within an *imaginary 2d coordinate system* [4], using two basic movements:

- 1) rotate the hand around the wrist (“left/right”)
- 2) flex the instrumented finger (“up/down”)

Resting the wrist and finger on the surface has two important effects: first, it prevents fatigue of the arm and hand during the interaction. Second, it limits the variety of hand movements and promotes those that can be measured with our sensors. In fact, we have only seen a small number

of ways in which users can move their finger so that the system fails. These are enumerated in the Discussion below.

The concept of *imaginary coordinates* is borrowed from [4]. We use the term loosely since the main application studied in this paper (pointing) is not screen-less but includes visual feedback. However, our design does not preclude screen-less operation, for example, for gestures.

We refer to our imaginary coordinate system as *wrist coordinates*. At the beginning of the interaction the wrist coordinate system (\mathbf{x}, \mathbf{y}) is established on the surface such that its origin is at a fixed distance w to the wrist, and the finger points in the y (“up”) direction (Fig. 2, right). The physical size of the unit square in wrist coordinates is defined by the user’s comfortable motion range. Both the physical size and the origin’s distance to the wrist w are defined during the calibration procedure described below.

MODEL

To recover fingertip positions from the sensor readings we use the model illustrated in Fig. 2 (right). We assume that the center of the wrist is fixed in space, creating an anchor point A around which the user rotates the hand during the interaction. A left/right rotation of the hand will move the fingertip along a circle with radius r and change the angle Φ . Flexing and extending the finger will move the fingertip further and closer to the wrist, changing r .

Clearly, if we know Φ and r , we can recover the fingertip position in wrist coordinates \mathbf{x} and \mathbf{y} . By design, determining Φ amounts to integrating the gyroscope output $d\Phi$ over time. Specifically, we integrate $d\Phi$ from the beginning of interaction, when $\Phi = 0$. For the short interactions tested in this paper (less than 20 seconds) gyro drift was not a problem, but it may be necessary to correct for drift with a magnetometer for other longer interactions. Determining r involves an additional step. In general, the mapping between the measured quantity \mathbf{d} and the fingertip radius r is determined by several nonlinear effects, including kinematics of the flexing movement, the IR brightness falloff, and nonlinearities in the IR detector. The mapping can be estimated with a calibration procedure, e.g. by letting the user move their finger along a set of known radii r , and recording the corresponding \mathbf{d} values.

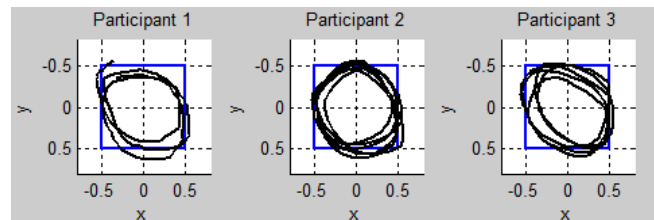


Figure 3. Calibration data (black line) from three users mapped to wrist coordinates (blue square).

By experimenting with different calibration schemes we found that the mapping between \mathbf{d} and r can be approximated by a linear model without losing much

accuracy. For the scope of this paper the added value of a simpler and more robust calibration procedure seemed to outweigh the small distortions coming from the linear approximation. Moreover, we noticed that the range of wrist angles Φ is typically small, which lets us approximate $\mathbf{x} \sim \Phi$. Overall, our model for mapping sensor readings to wrist coordinates is simply linear: $\mathbf{x} = \mathbf{a} * \Phi$ and $\mathbf{y} = \mathbf{b} * \mathbf{d} - \mathbf{w}$.

CALIBRATION

With the linear model the calibration process reduces to finding the sensor values \mathbf{d} and Φ that correspond to the center and physical size of the wrist coordinate system. To calibrate the system the user continuously traces a freehand circle on a flat surface (many shapes would suffice, but we found users could produce circles consistently and comfortably). No visual guide or feedback is provided. The user is instructed to choose the vertical position and size of the circle such that the motion covers most of the comfortable range, but does not require full extension of the finger (which would be outside the proximity sensor range).

Once the user finds a comfortable circle location and diameter (typically 3-5cm), five seconds of sensor data are recorded and the calibration parameters are computed as: $\mathbf{a} = 0.35/\text{SD}(\Phi)$, $\mathbf{b} = 0.35/\text{SD}(\mathbf{d})$, and $\mathbf{w} = \mathbf{b} * \text{mean}(\mathbf{d})$. Here, SD means standard deviation and the 0.35 factor ($\approx 1/2\sqrt{2}$) is the inverse SD of a sine wave signal with peak-to-peak amplitude 1. The rationale is that since the user traces a circle, Φ and \mathbf{b} will be sine waves, and so this scale factor maps the user's circle to the unit square (the physical size) of the wrist coordinate system. The mapped calibration circles of three users are shown in Fig. 3. The fact that these shapes are recognizable as circles supports the validity of our linear approximation.

EVALUATION

We tested the pointing performance of *LightRing* in a reciprocal pointing task [8]. We showed black circular targets in a white 22x22cm square (mapped to the wrist coordinate system) on a 23" LCD display at 60cm distance. Participants used their non-dominant hand to select targets by pressing a hardware push button. We tested four angles (0°, 45°, 90°, 135°), two distances (9.6cm, 19.2cm), three widths (1.1cm, 2.2cm, 4.4cm), overall: 3x2x3=24 trials. Each trial consisted of 10 repetitions. We further tested two conditions: using *LightRing* on a desk while sitting down, and using it on the side of the leg while standing. For standing, the display was elevated to eye level. We ran two blocks of 24 trials for each condition. The condition order was counterbalanced between subjects. This yielded 960 data points per subject.

Average movement times (*MT*) were 1.2s (SD 0.20s) for desk and 1.1s (SD 0.12s) for leg. Error rates (% clicks outside target) were 5.9% (SD 2.4%) for desk and 7.6% (SD 4.8%) for leg. We also computed throughput as $TP = \text{IDe}/\text{MT}$, where $\text{IDe} = \log_2(D/\text{We} + 1)$ (in bits) is the effective index of difficulty, D is the target distance, and

We is 4.133 times the standard deviation of participants selection coordinates [8]. Throughput was 2.9 bps (bits/second) (SD 0.31) for desk and 2.8 bps (SD 0.36) for leg. Neither of these differences was significant. Fig. 4 (top row) shows *MT* and Error rates per $\text{ID} = \log_2(D/W)$ (W =actual target width). The correlation coefficient was $\rho=0.86$ for the desk condition and $\rho=0.91$ for the leg condition, indicating reasonable agreement with Fitts' law.

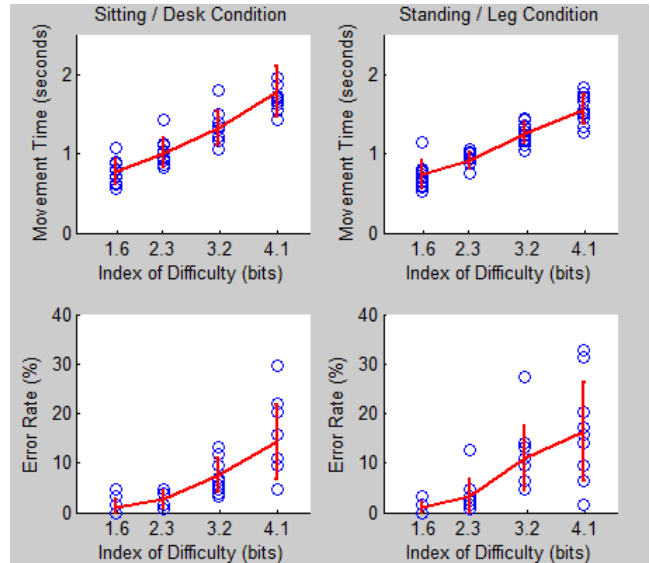


Figure 4. Pointing performance vs. Index of Difficulty (ID), while sitting (left column) and standing (right column). Top row: movement time, bottom row: Error rate. A blue circle denotes average performance for one participant. The red line shows the average over participants with one SD error bars.

A perhaps surprising result was that participants achieved similar performance for leg and desk. We expected lower performance in the leg condition due to the uneven surface of the clothing and due to a higher cognitive demand caused by performing the input with the hand pointing down to the floor. Instead, some subjects reported that the leg condition was “easier” due to less friction compared to the tabletop.

We also analyzed learning effects. There were no significant differences in *MT*, Error rate, or *TP* between the first and second block of either condition. However, over the course of all four blocks (both conditions, counterbalanced for order), *MT* changed significantly ($F(3,9)=5.2$, $p<0.01$). A post-hoc Tukey's test ($p<0.05$) revealed that *MT* was higher during the first block (1.3s) than during the following three blocks (1.1s). Similarly, *TP* changed significantly between blocks ($F(3,9)=5.05$, $p<0.01$), with *TP* lower during the first block (2.6 bps) than following blocks (2.9-3.0 bps). Error rates did not change significantly between blocks ($F(3,9)=0.83$, $p=0.48$).

DISCUSSION

The current sensor design is based on the assumption that there is a monotonic relationship between \mathbf{r} and \mathbf{d} : the closer the fingertip to the wrist, the higher the IR detector

output \mathbf{d} . However, \mathbf{d} merely reflects the angle of the *proximal interphalangeal (PIP)* joint, which is not the only joint that can move during finger flexion. In practice, we have seen two cases where this causes our system to fail: first, if pressure is applied the *distal interphalangeal (DIP)* joint can “snap” back and forth, changing \mathbf{d} , but not \mathbf{r} (Figure 5, left). Second, if the fingertip is moved by fully extending the finger and rotating it around the *metacarpophalangeal joint (MCP)* (Figure 5, right), \mathbf{r} changes, but \mathbf{d} does not (besides \mathbf{d} being out of range of the IR sensor if the finger is fully extended).

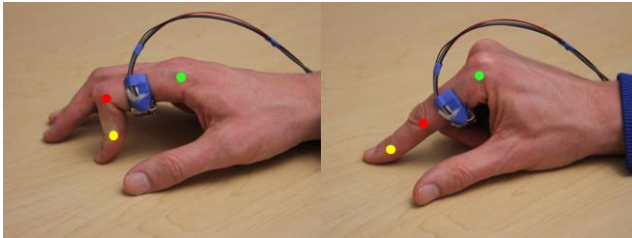


Figure 5. Failure cases and the finger joints involved (green=MCP, red=PIP, yellow=DIP): (Left) applying pressure. (Right) keeping the finger fully extended.

Interestingly, once users are instructed to avoid 1) pressure, and 2) fully extending their finger, the system appears to work fine. A possible explanation can be found in the *Digits* system [6], a wrist-worn that is sensor able to reconstruct the full 3d hand pose. *Digits* assumes that during *natural finger flexion* PIP, DIP, and MCP not only work in concert, but their angles are *related by fixed ratios at all time*, a motion that would satisfy our monotonicity assumption as well. Thus, although natural flexion occurs in mid-air, not on a surface, we conjecture that as soon as users avoid pressure and full extension, they switch to a gentler motion, closer to natural flexion, which has the above properties and thus makes *LightRing* work.

We also observed that in order to move the fingertip left and right some users rotated the finger around the MCP joint instead of rotating the hand around the wrist. Please note that this does not violate our modelling assumptions: it merely shifts the “wrist” anchor point \mathbf{A} (Fig. 2, right) to the actual point of rotation, i.e. the MCP joint. The same argument holds for the elbow as rotation anchor.

The linear calibration model turned out to be very robust. Once calibrated, *LightRing* can be slightly rotated around the finger, even taken off and on again, without requiring recalibration. Larger accidental rotations would have to be addressed explicitly, however, e.g. by giving the ring an asymmetric shape (like an engagement or class ring) so that the user can feel the orientation. Or, multiple proximity sensors could be placed around the ring to recover the signal in any orientation (using techniques like *iRing* [9] to determine absolute rotation angle).

In this note we have not provided a solution for initiating or “unlocking” the interaction. One way would be to use a button on the ring. Alternatively, the calibration procedure

itself could be used as an unlocking mechanism: the user could simply trace, say, three circles on the surface. This would also allow for the size the wrist coordinate system to adapt to different applications or body poses (which may differ in terms of comfortable motion ranges). In systems with visual feedback (i.e. a cursor), another possibility is to keep the interaction “always on” by clamping the cursor position at the screen edges, so that when the user moves towards a screen edge, any further movement in that direction will simply drag the wrist coordinates along.

CONCLUSION AND FURTHER WORK

We have introduced *LightRing*, a novel finger-worn sensor for digitizing subtle, fine-grained fingertip movements on any surface. User data indicates that the system is accurate and fast enough—about 3 bits/second pointing throughput after minimal practice—to enable real-world applications on the go that would traditionally require a mouse or touchpad. For example, *LightRing* could enable mobile text entry with smart glasses, or browsing the web on a distant display. To explore these scenarios in an ecologically valid manner we are planning to make *LightRing* wireless and add a capacitive button for selecting targets. Moreover, we are interested in investigating applications without visual feedback (and potentially eyes-free), such as recognition of 2d gestures.

ACKNOWLEDGMENTS

We would like to thank Scott Saponas, Desney Tan, and Mike Sinclair for insightful discussions.

REFERENCES

1. Ahmad, F. and Musilek, P. UbiHand: a wearable input device for 3D interaction, SIGGRAPH 2006 (poster)
2. Chan, L., et al. FingerPad: private and subtle interaction using fingertips. UIST 2013.
3. Chen, K., et al. uTrack: 3D input using two magnetic sensors. UIST 2013.
4. Gustafson, S., et al. Imaginary interfaces: spatial interaction with empty hands and without visual feedback. UIST 2010.
5. Howard, B. and Howard, S. Lightglove: Wrist-worn virtual typing and pointing. IEEE ISWC 2001
6. Kim, D., et al. Digits: freehand 3D interactions anywhere using a wrist-worn gloveless sensor. UIST 2012.
7. Lam, A., et al. MIDS: micro input devices system using MEMS sensors. IEEE Intelligent Robots and Systems 2002.
8. MacKenzie, I. S. Fitts' law as a research and design tool in human-computer interaction. *Hum.-Comp. Interact.* 7(1) 1992.
9. Morris, D., et al. Emerging Input Technologies for Always-Available Mobile Interaction. *Foundations and Trends in Human-Computer Interaction* 4 (4) 2011.
10. Niikura, T. et al. Anywhere surface touch: utilizing any surface as an input area. AH 2014.
11. Ogata, M., et al. iRing: intelligent ring using infrared reflection. UIST 2012.
12. Sturman, D. J., and Zeltzer, D. A survey of glove-based input. *Computer Graphics and Applications* 1994.
13. Yang, X., et al. Magic finger: always-available input through finger instrumentation. UIST 2012.